Scale-up of cluster beam deposition to the gram scale with the matrix assembly cluster source for heterogeneous catalysis (propylene combustion)

Rongsheng Cai (iD), Lu Cao, Ross Griffin, Sarayute Chansai, Christopher Hardacre, and Richard E. Palmer (iD)

View Online   **Export Citation**   **CrossMark**

Scale-up of cluster beam deposition to the gram scale with the matrix assembly cluster source for heterogeneous catalysis (propylene combustion)

Rongsheng Cai,[1] (iD) Lu Cao,[2] Ross Griffin,[2] Sarayute Chansai,[3] Christopher Hardacre,[3] and Richard E. Palmer[1,a] (iD)

AFFILIATIONS

[1] College of Engineering, Swansea University, Bay Campus, Fabian Way, Swansea SA1 8EN, United Kingdom

[2] Nanoscale Physics Research Laboratory, School of Physics and Astronomy, University of Birmingham, Birmingham B15 2TT, United Kingdom

[3] Department of Chemical Engineering and Analytical Science, The University of Manchester, The Mill, Sackville Street, Manchester M13 9PL, United Kingdom

[a] Author to whom correspondence should be addressed: r.e.palmer@swansea.ac.uk

ABSTRACT

Cluster beam deposition is a solvent-free method to prepare films of nanoparticles, one obvious application being heterogeneous catalysis. To address the problem of low cluster deposition rates, a novel cluster beam source, the "Matrix Assembly Cluster Source" was invented recently. Following the proof of principle studies, here, we demonstrate a further scale-up by 2 orders of magnitude, equivalent to reaching a production of ~10 mg of clusters (Au_{100}) per hour. This allows the preparation of cluster-decorated powder catalysts at the gram scale, comfortably sufficient for practical catalysis studies of novel materials at the research level, as demonstrated here by the catalytic combustion of propylene.

Preformed and precisely controlled clusters directly deposited onto suitable supports represent attractive new systems for heterogeneous catalysis research.[1–3] Cluster beam deposition (CBD) offers a solvent-free (and thus an effluent-free) route to the preparation of novel catalytic systems.[4] At one extreme, with the help of a time-of-flight mass filter, the clusters produced can achieve even single atom precision.[5,6] However, the mass selection process only allows a small proportion of the clusters synthesized (in gas or a matrix phase) to be deposited.[2,7] Thus, a new type of high flux cluster beam source, the Matrix Assembly Cluster Source (MACS), was developed recently; the technique is scalable but retains ~10% definition in the cluster size.[8–11] This novel technique is based on the assembly of atoms in a metal-loaded cryogenically cooled rare gas matrix initiated by ion beam impact. To date, the cluster deposition rate appears to depend linearly on the ion beam current, suggesting linear scaling. In previous reports,[8,12] we demonstrated the principle of cluster formation and deposition (for silver and gold clusters) and an instrument which scales the method to reach up to ~100 μg of clusters (Au_{100}) per hour.[12] This latter cluster beam intensity was equivalent to a current of ~100 nA (thus a scale-up of 3 orders of magnitude compared with a traditional size-selected cluster beam source).[5] However, this scale, which is sufficient to decorate planar surfaces, for, e.g., biochips, is still too low (about 100 times) for the comfortable decoration of powder catalysts at the gram scale.

In this paper, we report a new instrument enabling a further scale-up of the cluster flux by another 2 orders of magnitude (to around 10 mg of Au_{100} clusters per hour) and demonstrate the

catalytic activity of silver (Ag) cluster catalysts on titanium dioxide (TiO_2) made by the MACS in propylene combustion under realistic reaction conditions. The successful scale-up approach allows the preparation of cluster-decorated catalyst powders at the gram scale with a good metal loading (e.g., 1 g of catalyst with 1 wt. % cluster loading produced within 1 h) for research and development at the test tube level.

Figures 1(a) and 1(b) show a photograph and schematic diagram of the up-scaled MACS-II system, which includes a cluster generation and deposition chamber and a sample load-lock chamber. The matrix is first prepared on a cryogenically-cooled (Sumitomo Heavy Industries, Cryocooler, CH-204) oxygen-free copper block (1-in. square) with a typical temperature of 20 K by co-condensing the rare gas (Ar) and metal atoms evaporated from a thermal evaporator (CreaTec: HTC) in the main chamber. Then, it is sputtered by an Ar ion beam (at an angle of 45° to the matrix) to generate a beam of clusters. The diagram in Fig. 1(c) demonstrates the sputtering process. The Ar ion beam employed generates a cascade of ion impacts in the solid matrix causing atoms to move around, to stick together, and to ripen in a dynamic environment. Eventually, the ripened clusters will be sputtered out by successive ion impacts.[9] During deposition, the vibration cup (stainless steel, Teer Coatings Ltd.), containing a powder which is agitated mechanically by an unbalanced motor, is located close to the matrix support to harvest the clusters produced. A water-cooled quartz crystal microbalance (QCM) is used to measure the cluster flux. The Ar ion source employed in the MACS-II (Tectra, Gen2 plasma source) can deliver an Ar ion beam of up to 3 mA, which is about 100 times higher than that delivered by the ion source used in a previous report.[12]

To investigate the performance of the MACS system, the generated cluster beam profile was first calibrated by collecting Ag clusters onto a series of transmission electron microscope (TEM) grids positioned as shown in Fig. 2. A matrix with a ~3% metal concentration (the number of Ag atoms compared with that of Ar atoms) was prepared for 20 min (thickness: ~300 nm). Then, an Ar ion beam (current: ~1 mA, energy: 1 keV) was introduced to sputter the matrix. The distance between the TEM grids is 2 cm, and the TEM grid holder is placed 5 cm away from the center of the matrix support. After deposition for 10 s, the samples collected were characterized by a JEOL JEM 2100F aberration-corrected scanning transmission electron microscope (STEM) to obtain the cluster beam profile, as shown in Figs. 2(b) and 2(c). The high-angle annular dark field (HAADF) STEM images in Fig. 2(b) show that the cluster density decreases when collected further away from the matrix support. If we assume the cluster beam profile to be symmetric, we find this profile can be fitted by a Gaussian curve with the maximum cluster density in the middle, as seen in Fig. 2(c). Based on the 2D cluster profile, the entire cluster beam shape (3D profile) could also be deduced. Ag cluster size distribution was obtained in a straightforward fashion from HAADF-STEM images of deposited clusters. In this experiment, to avoid depleting the matrix, Ag clusters were produced in a continuous mode (the evaporator is left open to continually dose the matrix with metal during sputtering). Figure 3 shows the distribution as a function of time over a 50 min deposition run. It can be seen that the mean cluster size is around 1.5 nm (thus containing around 120 Ag atoms) and does not change significantly with sputtering time.

The cluster deposition rate (in terms of the mass of Ag) was measured directly over 1 h with the QCM (0.8 cm in diameter), which was placed under the matrix support at a distance of 5 cm from the center. Clearly, the size of the QCM is significantly smaller than the width of the cluster distribution, as shown in Fig. 2. The entire cluster beam intensity emerging from the matrix was
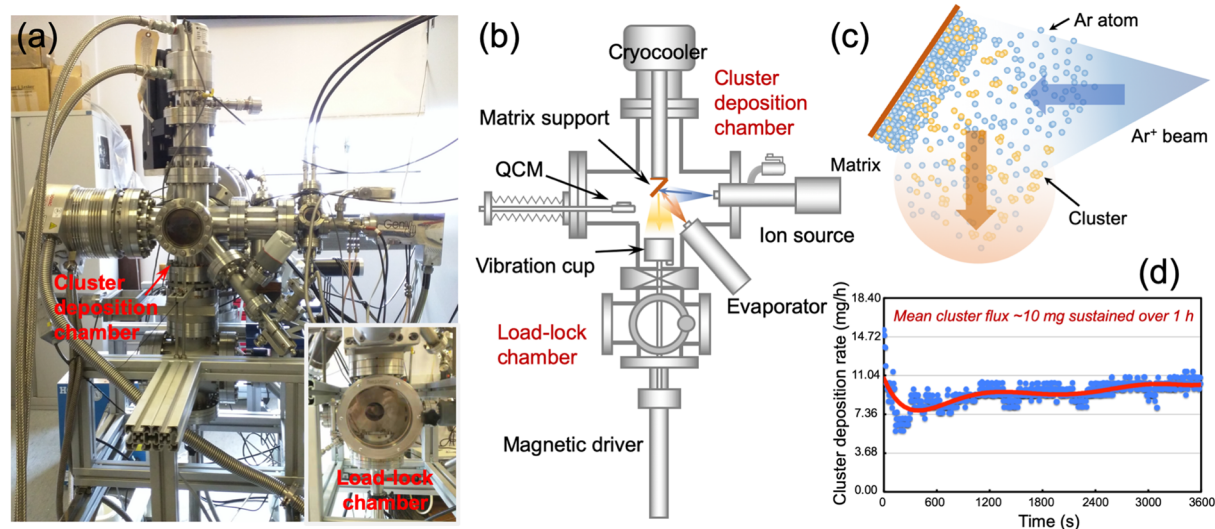

FIG. 1. Up-scaled MACS-II cluster beam deposition source: (a) the photograph and (b) the schematic diagram of the MACS system with components labeled in (b), (c) the schematic of the sputtering process, and (d) demonstration of the cluster deposition rate (Ag cluster) as a function of sputtering time. Related parameters—continuous mode; initial matrix thickness: ~300 nm; ~3% metal concentration; 20 K; and Ar⁺ beam current incident on the matrix at 1 keV, ~1 mA.
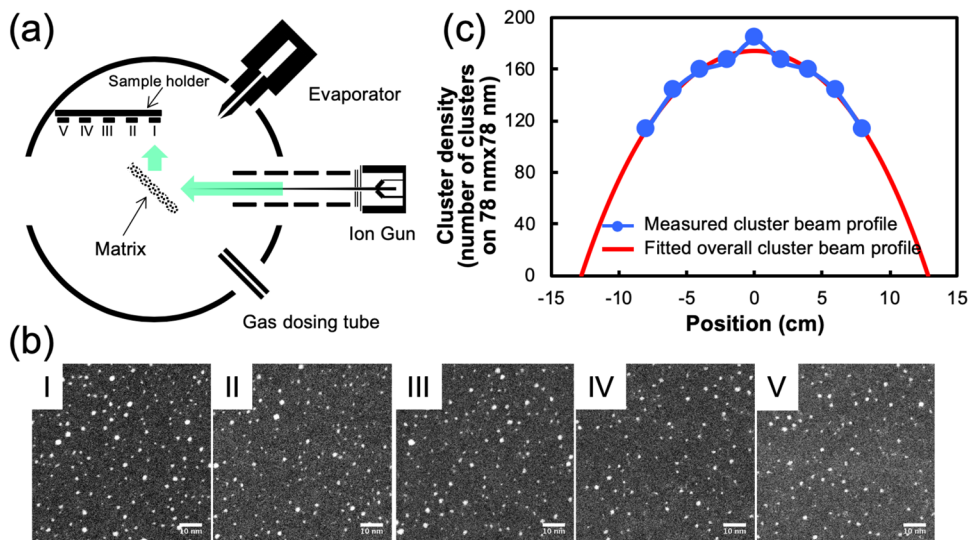
FIG. 2. Calibration of the MACS cluster beam profile by deposition of Ag clusters onto a series of TEM grids: (a) the schematic diagram of the experimental setup; a sample holder with five TEM grids was placed beneath the matrix support at a distance of 5 cm from the center of the matrix support, (b) typical HAADF STEM images of the Ag clusters collected on the five different grids, and (c) the measured cluster density profile and a Gaussian fit. Related parameters—matrix thickness: ~300 nm; ~3% metal concentration; ~20 K; Ar$^+$ beam current incident on the matrix at 1 keV, ~1 mA; and 10 s deposition time.

calculated by integrating the total signals across the fitted beam profile and is shown in Fig. 1(d). Although the cluster intensity exhibits some modest fluctuations, over the period of 1 h, it is quite stable. The mean cluster flux is around 12 μA, equivalent to ~10 mg of clusters (Au$_{100}$) per hour. Compared with a traditional size-selected cluster beam source (cluster current ~0.1 nA), the MACS-II presented in this work would increase the cluster flux by 5 orders of magnitude, assuming all the clusters in the beam profile were collected. In practice, our powder cup (dimension: 5.5 cm in diameter) captures about 60% of the total available cluster beam intensity.

To demonstrate the viability of the MACS method for the production of powder catalysts, which can be investigated under realistic reaction conditions, we conducted test experiments on the

catalytic combustion of hydrocarbon. This is one of the key ways to diminish automotive emissions[13,14] as well as a model reaction in heterogeneous catalysis.[15] The scale-up of the MACS enabled us to prepare cluster-decorated powder catalysts at the gram scale. Specifically, Ag clusters were separately deposited onto TiO$_2$ and Al$_2$O$_3$ powder supports (denoted as Ag/Al$_2$O$_3$ and Ag/TiO$_2$) and used for propylene combustion. Figures 4(a) and 4(b) show typical HAADF STEM images and the corresponding cluster size distribution for densely decorated Al$_2$O$_3$ and TiO$_2$ supports, respectively. Ag clusters are observed on the supports. Besides small clusters of ~2 nm, larger clusters are also visible, likely due to the aggregation of clusters on the powder surface. The two cluster samples show similar cluster size distributions with the peak size at 5.0 nm for Ag/Al$_2$O$_3$ and 4.2 nm for Ag/TiO$_2$. However, it should be noted that
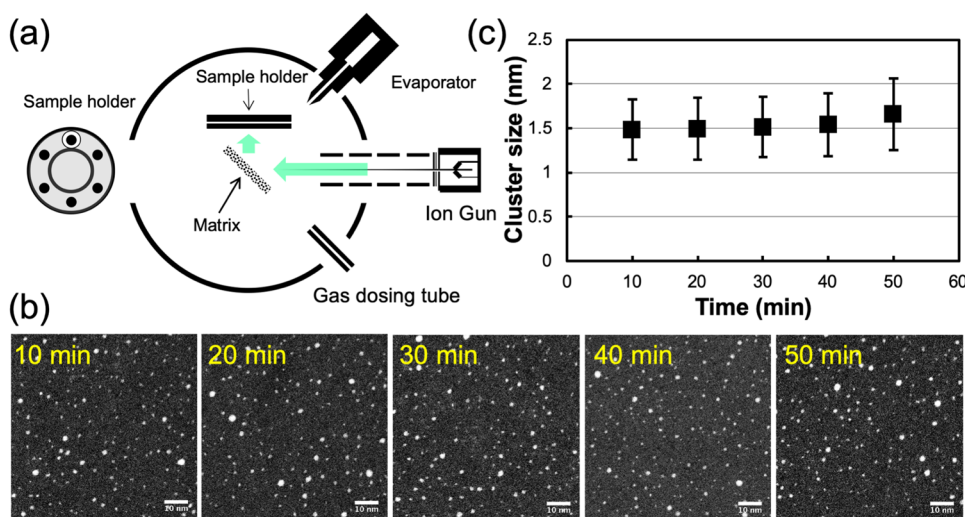

FIG. 3. Calibration of the cluster size evolution with sputtering time: (a) the schematic diagram of the experimental setup, (b) typical HAADF STEM images of the Ag clusters collected at five different sputtering times for 10 s, and (c) the plot of the cluster mean size vs sputtering time. Related parameters—continuous mode; initial matrix thickness: ~300 nm; ~3% metal concentration; ~20 K; Ar$^+$ beam current incident on the matrix at 1 keV, ~1 mA; and 10 s deposition time.
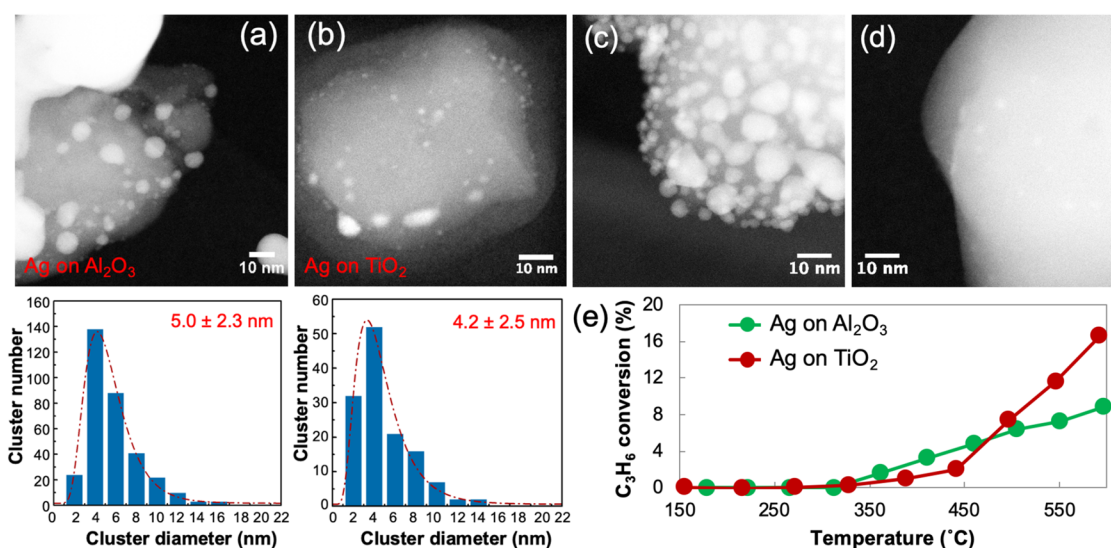
FIG. 4. Ag cluster catalysts made with the MACS-II demonstrated in propylene combustion: [(a) and (b)] typical HAADF STEM images and corresponding cluster size distributions of Ag clusters on Al_2O_3 and TiO_2, respectively, [(c) and (d)] HAADF STEM images of the support particles which are (c) fully decorated with clusters and (d) nearly without clusters, respectively, and (e) Ag cluster activities in propylene combustion. Both Ag/Al_2O_3 and Ag/TiO_2 exhibit activity above 300 °C.

on the microscope scale, the loading of the clusters on the powders is very uneven. Powder particles fully covered with Ag clusters were observed together with some particles nearly without any clusters, as seen in Figs. 4(c) and 4(d). The calculated local cluster loading varies from zero to as high as ~37 wt. %, if we assume all the particles to be spherical. The non-uniform decoration of clusters on the powder support is a consequence of less than ideal mixing of the powders during CBD. The agitation method needs to be improved, and recently, we have added with an *in situ* stirrer to address the problem. Nevertheless, the samples do allow unambiguous demonstration of the catalytic activity of the materials generated by the novel method.

The obtained oxide-supported Ag cluster catalysts were directly used in the propylene oxidation reaction [100 mg catalysts, 720 ppm NO, 4340 ppm (as C1) of C_3H_6, 4.3% O_2, 7.2% H_2O, 7.2% CO_2, and balance Ar, flow rate: 100 cm^3 min^{-1}]. Figure 4(e) shows the catalysis results. It can be seen that the propylene conversion starts when the temperature reaches around 300 °C for both types of materials, Ag/Al_2O_3 and Ag/TiO_2, above which the conversation rate is elevated. The Ag/TiO_2 cluster catalyst exhibits a slightly higher activity above ~480 °C, which may be due to the smaller cluster sizes on the supports. It should be mentioned that although the performance of the cluster-decorated catalysts produced with the MACS cannot compete with the reference samples (made by other chemical methods) that are reported in the literature (materials and supports are not optimized) at the moment,[16,17] this method still provides a way to explore the original catalytic activity of "ligand-free" clusters. This is the first demonstration of actual cluster catalysts made by the MACS in gas phase catalytic reactions.

In this paper, we have demonstrated that by using a higher sputtering current and corresponding scale-up, a scaled-up MACS system could achieve a cluster production rate equivalent to ~10 mg of clusters (Au_{100}) per hour, an increase of 5 orders of magnitude compared with the cluster production of a traditional size-selected cluster beam source. The increased cluster flux has allowed us to make practical Ag cluster catalysts on Al_2O_3 and TiO_2 powder supports at the gram scale. We found both cluster-decorated materials exhibited catalytic activities in the propylene combustion reaction above 300 °C. This successful scale-up shows that cluster beam deposition can be applied to the creation of a new generation of heterogeneous catalysts for practical R&D applications under realistic conditions.

REFERENCES

[1] S. Vajda and M. G. White, ACS Catal. **5**, 7152 (2015).

[2] R. E. Palmer, R. Cai, and J. Vernieres, Acc. Chem. Res. **51**, 2296 (2018).

[3] R. Cai, P. R. Ellis, J. Yin, J. Liu, C. M. Brown, R. Griffin, G. Chang, D. Yang, J. Ren, K. Cooke, P. T. Bishop, W. Theis, and R. E. Palmer, Small **14**, 1703734 (2018).

[4] J. Xu, S. Murphy, D. Xiong, R. Cai, X.-K. Wei, M. Heggen, E. Barborini, S. Vinati, R. E. Dunin-Borkowski, R. E. Palmer, and L. Liu, ACS Appl. Energy Mater. **1**, 3013 (2018).

[5] S. Pratontep, S. J. Carroll, C. Xirouchaki, M. Streun, and R. E. Palmer, Rev. Sci. Instrum. **76**, 045103 (2005).

[6] T. Momin and A. Bhowmick, Rev. Sci. Instrum. **81**, 075110 (2010).

[7] E. C. Tyo and S. Vajda, Nat. Nanotechnol. **10**, 577 (2015).

[8] R. E. Palmer, L. Cao, and F. Yin, Rev. Sci. Instrum. **87**, 046103 (2016).

[9] J. Zhao, L. Cao, R. E. Palmer, K. Nordlund, and F. Djurabekova, Phys. Rev. Mater. **1**, 066002 (2017).

[10] V. T. Oiko, T. Mathieu, L. Cao, J. Liu, and R. E. Palmer, J. Chem. Phys. **145**, 166101 (2016).

[11] R. Cai, N. Jian, S. Murphy, K. Bauer, and R. E. Palmer, APL Mater. **5**, 053405 (2017).

[12] P. R. Ellis, C. M. Brown, P. T. Bishop, J. Yin, K. Cooke, W. D. Terry, J. Liu, F. Yin, and R. E. Palmer, Faraday Discuss. **188**, 39 (2016).

[13] X.-C. Guo and R. J. Madix, J. Am. Chem. Soc. **117**, 5523 (1995).

[14] H. Wang, C. Chen, Y. Zhang, L. Peng, S. Ma, T. Yang, H. Guo, Z. Zhang, D. S. Su, and J. Zhang, Nat. Commun. **6**, 7181 (2015).

[15] A. Aznárez, A. Gil, and S. A. Korili, RSC Adv. **5**, 82296 (2015).

[16] F. Liu, Y. Sang, H. Ma, Z. Li, and Z. Gao, J. Nat. Gas Sci. Eng. **41**, 1 (2017).

[17] M. Montaña, M. Leguizamón Aparicio, M. Ocsachoque, M. Navas, I. de C. L. Barros, E. Rodriguez-Castellón, M. Casella, and I. Lick, Catalysts **9**, 297 (2019).